46
L. M. a. L.

[redacted]

TECHNICAL MEMORANDUMS

NATIONAL ADVISORY COMMITTEE FOR AERONAUTICS

No. 909

Prop.

THE THEORY OF CONTRA-VANES APPLIED TO THE PROPELLER

By Albert Betz

Ingenieur-Archiv
Vol. 9, No. 6, December 1938

1.5.1
1.5.4
1.4.6
1.5.2.1

Washington
September 1939

NATIONAL ADVISORY COMMITTEE FOR AERONAUTICS

TECHNICAL MEMORANDUM NO. 909

THE THEORY OF CONTRA-VANES APPLIED TO THE PROPELLER*

By Albert Betz

SUMMARY

The optimum circulation distribution and hence the maximum theoretical thrust obtainable for contra-vanes fitted behind propellers is markedly dependent on the number of guide vanes. The outer portions of the vanes, even if projecting considerably beyond the edge of the propeller slipstream, still contribute appreciably to this theoretical gain of thrust. But, owing to the always existing friction of the vanes, the limit of the optimum vane length lies at relatively small diameters. A large hub unloads the vanes. Hence, the guide vanes are best attached to suitable parts of the bodies which would, in any case, be subjected to the slipstream.

INTRODUCTION

On heavily loaded ship propellers and on airplane propellers with very high pitch, the spiral motion of the slipstream contains considerable kinetic energy which can be converted into effective energy to a large extent by contra-vanes.

In order to gain an idea of the effects obtainable by such an arrangement, the question may be raised as to the potential gain in energy in the best case with given distribution of the speed of rotation in the slipstream. Energy losses due to guide-vane drag are ignored for the present; they can be allowed for by separate appraisal, as on regular propellers.

If the design of the contra-vanes is free from all restrictions, the rotation can be obviated altogether

*"Zur Theorie der Leitapparate für Propeller." Ingenieur-Archiv, vol. IX, no. 6, December 1938, pp. 435-452.

through employment of infinitely many guide vanes, and so recover the total kinetic energy. But, if restricted to a finite number of vanes, as imposed in practice, the deflection effect between two vanes is less than directly at the vanes themselves. In consequence, there remain radial and tangential velocity residues. The energy is not fully recovered. A particularly interesting case is that of only two vanes set at 180°, as exemplified by the rudder aft of a ship's propeller or by the wing of an airplane. Moreover, the sternpost of a ship or the wing ahead of a propeller can be so designed as to act as inlet guide apparatus before the propeller. It then involves the problem of designing the sternpost or wing so as to leave a minimum of energy in the jet rotation.

GENERAL CONSIDERATIONS

Visualize the contra-vanes placed behind the propeller (discharge contra-vanes). Arranged before the propeller, the same circulation distribution is required. Hence the findings from the former are directly applicable to the latter. It needs only to be borne in mind that an entrance contra-vane causes a change in circulation about the propeller blades, and that the propeller slipstream resulting from this changed circulation distribution must be used as basis of the calculation.

The number of guide vanes is to be finite - no limitations being imposed at first as to size and shape of the vanes. They are to be determined for a maximum recovery of energy. The result will be theoretical guide vanes reaching from the axis to infinity which, of course, is impossible to realize but affords a good insight into the effect of the number of vanes. Further, it is attempted to study contra-vanes with finite radial length, where it is found that the outer parts of the contra-vanes are still comparatively very effective.

The rate of rotation in the slipstream is to be affected by the radius only; thus, the nonuniformity over a circumference due to the finite number of vanes is disregarded.

The action of the contra-vanes is as follows: The fluid has, aside from its axial velocity component v_1, the tangential component u_1, due to the spiral motion.

The resultant velocity is c_1 (fig. 1). We assume a lightly loaded propeller, so that the rise of axial velocity in the slipstream relative to the forward speed can be ignored - i.e., we can equate v within and without the jet to the speed of advance, and flying speed, respectively, and merely study the effect of the spiral velocity u. Placing in this flow a surface which deflects the passing particles to the velocity c_2, this surface is subject as airfoil to a force P at right angles to the mean flow direction (average of c_1 and c_2). This force has, in general, a component S in the direction of the ship's motion, which increases the propeller thrust and hence produces useful energy. This component becomes zero if the deflection becomes so severe that c_2 is turned through the same angle toward the direction of motion of the opposite side as c_1 (the energy of rotation then being the same as before). The force becomes negative if the deflection is more severe. The next problem is to establish the amount of deflection necessary for a maximum thrust component; that is, greatest power gain.

The deflection depends upon the magnitude of the circulation around the blade. The optimum is reached if a small increase in circulation no longer brings a rise in thrust.

According to the methods (reference 1) known from the propeller theory, it is expedient to apply this small circulation increment, not at the blade itself but far downstream from it and on streamlines emanating from the blade area. The momentum and energy conditions are then the same as if the increment had been applied at the blade itself. One advantage accruing from it is, that the increment no longer affects the flow around the remaining blade, hence restricts consideration of the effect of the flow downstream from the wing to the little (circulation-increasing) wing, but not the reaction of this little wing on the remainder. With such an auxiliary winglet, it is always possible to recover a thrust component and hence a gain in energy from the flow as long as the flow maintains a transversely directed velocity component u. The contra-vanes have, accordingly, extracted the maximum of power from the spiral motion of the slipstream when the streamlines from the trailing edge at some length behind the contra-vanes no longer disclose a tangential velocity component. This condition could be realized in very simple fashion by extending the surfaces of the contra-vanes rearward as long, rigid, flat surfaces parallel to the axis, although this is ruled out in practice on account of the excessively great surfaces.

PRINCIPLES FOR COMPUTING THE CIRCULATION DISTRIBUTION

The next problem is the circulation distribution along the guide vanes for best efficiency. As from every airfoil, a surface of discontinuity emanates from the trailing edge of the guide vanes. If $\Gamma = \Gamma(r)$ is the circulation around a guide vane at distance r from the axis, the circulation around a strip of the vortex surface between r and $r + dr$ is

$$\Gamma' dr = \frac{\partial \Gamma}{\partial r} dr \tag{1}$$

Now the field of this vortex surface must be such that the points located on it yield transverse velocities which are equal and opposite to the tangential velocities produced by the propeller, so that they are exactly canceled by the field of the vortex surface.

The velocities along the vortex surface are on one side outwardly, on the other inwardly, directed. If this longitudinal velocity is w, the increment of velocity in the vortex surface, and hence the circulation per unit length is

$$\Gamma' = 2w \tag{2}$$

If $u = u(r)$ is the distribution of the transverse velocities to be removed, the problem consists in finding a potential motion, for which the normal velocity $-u$ along the edge is given and the tangential velocity w is to be defined. This is a well-known boundary value problem of potential theory.

A contra-vane with n blades can, by a conformal transformation

$$\zeta = z^{n/2} \quad \text{or} \quad \zeta = z^n \tag{3}$$

be changed to another of two- or one-blade. Hence the findings for a two- or one-blade contra-vane are comparatively easily applied to contra-vanes of any number of blades.

The distribution of the tangential velocity u over the propeller radius R may be very different. For a lightly loaded propeller without contra-vanes, the distribution for minimum energy loss is (reference 2)

$$u = w \frac{v\, r\, \omega}{v^2 + (r\, \omega)^2} \tag{4}$$

where v is the speed

ω, angular velocity of propeller

w, a constant dependent on the thrust loading

For a propeller with contra-vanes, the best distribution obtains when propeller thrust and contra-vanes together are uniformly distributed over the whole propeller disk area (simple slipstream theory). Each stream filament then receives the same energy increment. This condition yields

$$u = v\, k\, \frac{R}{r} \tag{5}$$

whereby

$$k = \lambda\, \frac{c_s}{2\eta_p} \tag{6}$$

and

$$c_s = \frac{S}{\frac{\rho}{2}\, F\, v^2} \tag{7}$$

the load coefficient of the propeller, η_p the propeller efficiency, and $\lambda = \frac{v}{R\omega}$, the coefficient of advance. (S is the thrust, ρ, fluid density, $F = R^2\pi$, swept-disk area for propeller radius, R.)

This simple distribution is to serve as basis hereinafter. It will be observed, of course, that it affords an infinite tangential velocity $(u \longrightarrow \infty)$ in the propeller axis $(r \longrightarrow 0)$, which is impossible to realize in practice. But for contra-vanes with hubs, this difficulty is obviated.

CONTRA-VANES WITH UNLIMITED OUTSIDE RADIUS

The outside radius of the propeller jet is R, the contra-vanes have n blades mounted on a hub of radius r_o.

By reflection on the hub, the flow can be visualized as continuing within the hub (fig. 2). In this reflection, a point P at distance r from the axis defines a reflected point P_i on the same radius at distance

$$r_i = \frac{r_o^2}{r} \tag{8}$$

from the axis. The outside boundary of the slipstream has, accordingly, as reflection, an inside boundary of radius

$$R_i = \frac{r_o^2}{R} \tag{9}$$

Introducing the nondimensional quantities

$$\xi = \frac{r}{R}, \qquad \xi_o = \frac{r_o}{R} \tag{10}$$

we find

$$\frac{r_i}{R} = \frac{\xi_o^2}{\xi} \quad \text{and} \quad \frac{R_i}{R} = \xi_o^2 \tag{11}$$

If at point P the tangential velocity is u, and the radial velocity is w, the reflection in point P_i gives the tangential and radial velocities at

$$u_i = - u \frac{\partial r}{\partial r_i} = u \left(\frac{r}{r_o}\right)^2 = u \left(\frac{r_o}{r_i}\right)^2 \tag{12}$$

$$w_i = w \frac{\partial r}{\partial r_i} = - w \left(\frac{r}{r_o}\right)^2 = - w \left(\frac{r_o}{r_i}\right)^2 \tag{13}$$

Since u is to be equal to $v\,k\,\frac{R}{r}$ in the slipstream outside of the hub, it is the reflected part of the flow

$$u_i = u \left(\frac{r_o}{r_i}\right)^2 = v\,k\,\frac{R}{r_i} \tag{14}$$

Hence the reflected velocity distribution is simply the continuation of the outside distribution according to the same law of distribution. Substitution of the hub by reflection simply affords a continuation of the jet inwardly up to inside radius R_i, according to the law of distribution of $u = v\,k\,\frac{R}{r}$.

The contra-vane is intended to reduce the tangential velocities behind the blades to zero. The reflection then presents zero velocity also. The guide vanes in the reflected part have the same purpose as in the outer part. The problem, accordingly, is to extract from an annular slipstream of R_i inside radius, and R outside radius, a maximum of energy by means of the guide vanes extending from $r = 0$ to $r = \infty$.

The calculation proceeds from a contra-vane with two blades, the findings from which are then easily applied to arrangements with any other number of blades by conformal transformation. This particular case of contra-vanes with two blades of infinite length is, as previously stated, of special significance for ships as well as airplanes.

Since with the two-blade arrangement, the surface of discontinuity downstream from the guide vanes extends from $r = -\infty$ to $r = +\infty$, the total space is divided into two congruent halves (fig. 3), so that the study may be restricted to one half-plane. In it the normal velocities along the boundary are predetermined; they are u and $-u$ on the lengths R_i to R, or from $-R_i$ to $-R$, respectively, and elsewhere, zero. Desired, are the correlated longitudinal velocities, w. They follow the sense of direction indicated in figure 3 at a point r_1 as

$$\left.\begin{aligned} w &= \int_{-\infty}^{+\infty} \frac{u(r)\,dr}{(r_1 - r)\pi} = \frac{vRk}{\pi}\left[\int_{-R}^{-R_i} \frac{-dr}{r(r_1 - r)} + \int_{R_i}^{R} \frac{dr}{r(r_1 - r)}\right] = \\ &= \frac{vk}{\pi}\left[-\int_{-1}^{-\xi_0^2} \frac{d\xi}{\xi(\xi_1 - \xi)} + \int_{\xi_0^2}^{1} \frac{d\xi}{\xi(\xi_1 - \xi)}\right] \end{aligned}\right\} \qquad (15)$$

For $r_1 > R$, it is

$$w(\xi_1) = \frac{vk}{\pi}\,\frac{1}{\xi_1}\,\ln\frac{(\xi_1 + 1)(\xi_1 - \xi_0^2)}{(\xi_1 - 1)(\xi_1 + \xi_0^2)} \qquad (16)$$

and for $r_0 < r < R$

$$w(\xi_1) = \frac{vk}{\pi}\,\frac{1}{\xi_1}\,\ln\frac{(1 + \xi_1)(\xi_1 - \xi_0^2)}{(1 - \xi_1)(\xi_1 + \xi_0^2)} \qquad (17)$$

The circulation around a guide vane being certainly zero at infinity, the circulation Γ for a point $r > R$ follows, according to equation (2), the integration with respect to w from this point to infinity at

$$(\xi) = 2 \int_r^\infty w(r_1)\, dr_1 = 2R \int_\xi^\infty w(\xi_1)\, d\xi_1 \qquad (18)$$

To make the integration the logarithmic expressions of equation (16) are developed in series

$$\ln \frac{\xi_1+1}{\xi_1-1} = 2 \left(\frac{1}{\xi_1} + \frac{1}{3\xi_1^{3}} + \frac{1}{5\xi_1^{5}} + \ldots\right) \qquad (19)$$

$$\ln \frac{\xi_1+\xi_o^{2}}{\xi_1-\xi_o^{2}} = 2 \left(\frac{\xi_o^{2}}{\xi_1} + \frac{1}{3}\,\frac{\xi_o^{6}}{\xi_1^{3}} + \frac{1}{5}\,\frac{\xi_o^{10}}{\xi_1^{5}} + \ldots\right) \qquad (20)$$

which gives

$$\Gamma(\xi) = \frac{4Rvk}{\pi}\left[f_1\left(\frac{1}{\xi}\right) - f_1\left(\frac{\xi_o^{2}}{\xi}\right)\right] \qquad (21)$$

whereby

$$f_1(x) = x + \frac{x^3}{3^2} + \frac{x^5}{5^2} \qquad (22)$$

This function f_1 is readily obtainable from figure 4, where $f_1(x) - x$ is illustrated. For $x = 1$, it leaves

$$f_1(1) = 1 + \frac{1}{3^2} + \frac{1}{5^2} + \ldots = \frac{\pi^2}{8} \qquad (23)$$

For the jet boundary, where $\xi = 1$, it accordingly leaves

$$(1) = \frac{1}{2}\, vkR\pi \left[1 - \frac{8}{\pi^2}\, f_1(\xi_o^{2})\right] \qquad (24)$$

For a point $r < R$ or $\xi < 1$, it is

$$\Gamma(\xi) = \Gamma(1) + 2R \int_\xi^1 w(\xi_1)\, d\xi_1 \qquad (25)$$

where w follows equation (17). Development of the logarithmic expressions, as in equations (19) and (20), leaves

$$\left.\begin{aligned}\Gamma(\xi) = \Gamma(1) + 4\,\frac{vkR}{\pi}\left[f_1(1) - f_1(\xi) - f_1(\xi_o) + f_1\left(\frac{\xi_o^2}{\xi}\right)\right] = \\ = \cancel{2}\,vkR\pi\left[1 - \frac{8}{\pi^2}\,f_1(\xi_o^2) - \frac{4}{\pi^2}\left\{f_1(\xi) - f_1\left(\frac{\xi_o^2}{\xi}\right)\right\}\right]\end{aligned}\right\} \qquad (26)$$

The circulation of the two blades at radius $r = R\xi$ together amounts to $2\Gamma(\xi)$ which, if compared with the total circulation of a system of infinite blade number, affording full recovery of spiral energy, would allocate to the latter in the range of $r_o < r < R$, a constant circulation

$$\Gamma_o = u\ 2r\pi = 2vkR\pi \qquad (27)$$

2 u r π

The ratio

$$\frac{2\Gamma(\xi)}{\Gamma_o} = 1 - \frac{8}{\pi^2}\,f_1(\xi_o^{\,2}) - \frac{4}{\pi^2}\left[f_1(\xi) - f_1\left(\frac{\xi_o^{\,2}}{\xi}\right)\right] \qquad (28)$$

$$\frac{2\Gamma(\xi)}{\Gamma_o} = \frac{4}{\pi^2}\left[f_1\left(\frac{1}{\xi}\right) - f_1\left(\frac{\xi_o^{\,2}}{\xi}\right)\right] \qquad (29)$$

for $\xi < 1$ and $\xi > 1$, respectively, is reproduced for several hub conditions ξ_o in figure 5. It will be seen that the blades must still have a powerful circulation far outside of the slipstream, to satisfy the optimum conditions.

Transforming an n-blade contra-vane with hub radius $r_o = R\,\xi_o$ in a jet radius R, to a two-blader, the hub radius becomes

$$r_{o2} = R\,\xi_{o2} = R\,\xi_o^{\,n/2} \qquad (30)$$

and for every other radius ξ changes to

$$\xi_2 = \xi^{\,n/2} \qquad (31)$$

The velocities in the particular points are as

$$\frac{u}{u_2} = \frac{n}{2} \xi^{n/2-1} \tag{32}$$

Since $u = k\, v/\xi$, $u_2 = (2/n)\, k\, v/\xi_2$. Hence k is replaced $(2/n)\, k$. Then the circulation in the corresponding points of the n-blade and the two-blade arrangement is identical. Consequently,

$$\Gamma(\xi, k) = \Gamma_2 \left(\xi_2, \frac{2k}{n}\right) = \Gamma_2 \left(\xi^{n/2}, \frac{2k}{n}\right) \tag{33}$$

and for $\xi < 1$, according to equation (26)

$$\Gamma(\xi) = \frac{2}{n} R\, k\, v\, \pi$$

$$\left[1 - \frac{8}{\pi^2} f_1(\xi_0^{\,n}) - \frac{4}{\pi^2} \left\{f_1(\xi^{n/2}) - f_1\left(\frac{\xi_0^{\,n}}{\xi^{n/2}}\right)\right\}\right] \tag{34}$$

Figures 6 to 8 contain the distribution of

$$\frac{n\Gamma}{\Gamma_0} = 1 - \frac{8}{\pi^2} f_1(\xi_0^{\,n}) - \frac{4}{\pi^2} \left[f_1(\xi^{n/2}) - f_1\left(\frac{\xi_0^{\,n}}{\xi^{n/2}}\right)\right] \tag{35}$$

for $\xi > 1$ and

$$\frac{n\Gamma}{\Gamma_0} = \frac{4}{\pi^2} \left[f_1\left(\frac{1}{\xi^{n/2}}\right) - f_1\left(\frac{\xi_0^{\,n}}{\xi^{n/2}}\right)\right] \tag{36}$$

for $\xi > 1$, for three, four, and six blades, as in figure 5. As the number of blades increases, the curves for the different hub sizes converge. Figures 9 to 12 give the same circulation distributions in different arrangement, which brings out the effect of blade number more clearly. The curves for $n = 10$ and $n = 20$ blades are also given.

For these circulation distributions the contra-vanes dispose of the spiral velocities u in the vortex surface behind the vanes. At the vanes themselves, the velocity is half of the original, i.e., $u/2$. This yields, according to Kutta-Joukowsky, a propulsion - i.e., a thrust gain of δS. For the n vanes together, it amounts per unit length, to

$$\frac{d(\delta S)}{dr} = \rho \frac{u}{2} n\Gamma \tag{37}$$

With complete utilization of the spiral energy, this thrust gain would amount to

$$\frac{d(\delta S_o)}{dr} = \rho \, \frac{u}{2} \, \Gamma_o \tag{38}$$

Thus the curves $n\Gamma/\Gamma_o$ of figures 5 to 12 present at the same time the distribution of the degree of utilization along the radius; but only the range within the slipstream ($\xi < 1$) is pertinent since $u = 0$ outside of it, and the circulation about the blades is not associated with any gain in thrust. The total gain is

$$\delta S = \rho \int_{r_o}^{R} \frac{u}{2} \, n \, \Gamma \, dr = \frac{n}{2} \, \rho \, R \int_{\xi_o}^{1} \overset{VK}{u(\xi)} \, \Gamma(\xi) \, d\xi \tag{39}$$

or, after inserting the values of u and Γ from equations (5) and (34):

$$\left.\begin{aligned} \delta S &= \rho \, R^2 \, \pi \, k^2 \, v^2 \int_{\xi_o}^{1} \frac{1}{\xi} \\ &\quad \left[1 - \frac{8}{\pi^2} \, f_1\left(\xi_o^{\,n}\right) - \frac{4}{\pi^2}\left\{f_1\left(\xi^{n/2}\right) - f_1\left(\frac{\xi_o^{\,n}}{\xi^{n/2}}\right)\right\}\right] d\xi \\ &= \rho \, R^2 \, \pi \, k^2 \, v^2 \, \Xi \end{aligned}\right\} \tag{40}$$

whereby

$$\Xi = \left[1 - \frac{8}{\pi^2} \, f_1\left(\xi_o^{\,n}\right)\right] \ln \frac{1}{\xi_o} - \frac{8}{n\pi^2}\left[f_2(1) - 2 f_2\left(\xi_o^{\,n/2}\right) + f_2\left(\xi_o^{\,n}\right)\right] \tag{41}$$

and

$$f_2(x) = \int_0^x \frac{1}{x} \, f_1(x) \, dx = x + \frac{x^3}{3^3} + \frac{x^5}{5^3} + \ldots \tag{42}$$

The function $f_2(x) - x$ is included in figure 4. For load coefficient c_s (7), the gain amounts to

$$\delta c_s = \frac{\delta S}{\frac{\rho}{2} R^2 \pi v^2} = 2k^2 \, \Xi = \frac{\lambda^2 c_s^2}{2 \eta_p^2} \, \Xi \tag{43}$$

where k is replaced by $\lambda c_s / 2\eta_p$, according to equation (6).

The total thrust gain recoverable from the spiral energy by infinite blade number, is

$$\delta S_o = \rho R^2 \pi v^2 k^2 \ln \frac{1}{\xi_o} \tag{44}$$

whence the maximum theoretical efficiency* of the n-bladed contra-vane becomes:

$$\left.\begin{aligned} \eta_m = \frac{\delta S}{\delta S_o} = \frac{\Xi}{\ln \frac{1}{\xi_o}} = 1 - \frac{8}{\pi^2} f_1(\xi_o^2) - \\ - \frac{8}{n \pi^2 \ln \frac{1}{\xi_o}} \left[f_1(1) - 2f_2(\xi_o^{n/2}) + f_2(\xi_o^n) \right] \end{aligned}\right\} \tag{45}$$

Figure 13 gives this efficiency plotted against the hub ratio ξ_o for different blade numbers n. It will be noted that for a fairly large hub with small blade number ($n = 2$), a fairly large portion of the spiral energy is lost. With small hubs the utilization is good, even by small blade number, so that greater blade numbers may, in general, be foregone. The proper choice of hub dimensions is discussed later on.

The calculation of the reaction moment of the guide vanes discloses the seemingly strange fact that for a small number of blades ($n = 2$), it exceeds the propeller torque (theoretically infinite). This is associated with the circulation about the blades extending surprisingly far beyond the edge of the slipstream, and results in the existence of a spiral motion downstream from the contra-vane of opposite rotation impulse to that upstream from it. In practice, this reversal of momentum is, of course, not reached

---

*Supplemented by the blade efficiency which expresses the losses due to blade resistance.

as a rule, but even so it must be borne in mind that the reaction moment of a propeller on an airplane can be very extensively balanced by the wing behind it.

CONTRA-VANES OF LIMITED OUTSIDE RADIUS

Since the guide vanes cannot, as assumed so far, be made of any length, it is of interest to establish the effect of a restricted radial extension of the blades. In itself, it might be suspected that the effectiveness of the guide-vane elements decreases with increasing axial distance, as there the tangential velocities, and so the recoverable energy become very small. But, according to previous studies on infinitely long vanes, the best circulation distribution with few blades still extends far beyond the jet boundary with quite considerable amounts (figs. 5 to 12). So, even if the blade portions beyond the jet boundary no longer yield a direct gain in thrust, since the tangential velocity is zero, they apparently still contribute perceptibly to the total result through their influence on the total flow. For structural reasons, the vanes naturally will be as short as possible, even if it means foregoing the best utilization of the spiral motion. To illustrate the consequences of such a restriction in vane length, the calculations were also carried out for vanes of finite length and, specifically, for the cases of vanes terminating inside and outside of the slipstream.

Let s = radius at which the guide vanes terminate, and R, the outside radius of the slipstream. The latter is of no significance for this problem so long as $s < R$. To compute the effect of such a contra-vane, the flow is again reflected at the hub. We proceed from a contra-vane having one vane (fig. 14), and then transfer the results to arrangements with n vanes by conformal transformation. To define the tangential velocities w from the normal velocities $u = v\,k\,\frac{R}{r}$ given along the guide vane and its image, the vane and its reflected continuation is conformably transformed on a circle at

$$\zeta = s_m + z + \frac{a^2}{z} \tag{46}$$

point

$$s_m = \frac{1}{2}\left(s + \frac{r_o^2}{s}\right) \tag{47}$$

being the center of the vane including its reflection. The length of the vane inclusive of its reflection, is

$$2l = s - \frac{r_o^2}{s} \tag{48}$$

The zero point of the z-plane is the center of the circle. The radius of the circle is

$$a = \frac{l}{2} = \frac{1}{4}\left(s - \frac{r_o^2}{s}\right) \tag{49}$$

For corresponding points of circle and vane become with

$$z = a\ e^{i\varphi}$$

$$\zeta = 2a \cos \varphi + s_m \tag{51}$$

The normal velocities on circle u_K are readily computable from the given normal velocities of vane u_S, since the velocity of correlated points of circle and vane is as

$$\frac{u_K}{u_S} = \left|\frac{d\zeta}{dz}\right| = 2 \sin\varphi \tag{52}$$

On the circle itself the tangential velocity w_K can be computed from the normal velocities u_K. In a point at angle φ_1 to the x-axis, we have:

$$w_K(\varphi_1) = \frac{1}{2\pi}\int_0^{2\pi} u_K(\varphi) \cot \frac{\varphi - \varphi_1}{2}\ d\varphi \tag{53}$$

The conversion on the ζ-plane conformable to equation (52) gives the desired tangential velocities w along the vortex band of the vane. In the evaluation of equation (53), two cases must be differential:

1) $s < R$, guide vane terminating wholly within slipstream.

2) $s > R$, guide vane extending beyond slipstream.

Again resorting to nondimensional quantities,

$$\xi = \frac{r}{R}, \qquad \sigma = \frac{s}{R}, \qquad \lambda = \frac{l}{R} = \frac{1}{2}\left(\sigma - \frac{\xi_o^2}{\sigma}\right) \tag{54}$$

With the corresponding indices, we find in the first case,

$$w_I = \frac{v\,k}{\sqrt{\lambda^2 - (\xi - \sigma_m)^2}}\left[1 - \frac{\sqrt{\sigma_m^2 - \lambda^2}}{\xi}\right] \tag{55}$$

Since here also

$$\frac{\partial \Gamma}{\partial r} = 2w$$

the circulation Γ at a point $r = R\xi$ follows at

$$\left.\begin{aligned} \Gamma_I(\xi) &= 2\int_r^s w\,dr = 2R\int_\xi^\sigma w\,d\xi \\ &= 2v\,k\,R\left[\arcsin \frac{1 + \left(\frac{\xi_o}{\sigma}\right)^2 - 2\left(\frac{\xi_o}{\sigma}\right)^2 \frac{\sigma}{\xi}}{1 - \left(\frac{\xi_o}{\sigma}\right)^2} + \right. \\ &\qquad \left. + \arcsin \frac{1 + \left(\frac{\xi_o}{\sigma}\right)^2 - 2\left(\frac{\xi}{\sigma}\right)}{1 - \left(\frac{\xi_o}{\sigma}\right)^2}\right] \end{aligned}\right\} \tag{56}$$

If $s > R$, velocity u_S within the jet boundary has the value $u_S = v\,k\frac{R}{r}$; without the jet boundary, it is zero. There is a point of discontinuity at the jet boundary, where it drops from $v\,k$ to zero. Similarly the distribution of the normal component u_K on the circle of the ζ-plane has a point of discontinuity at the four points corresponding to the jet boundary $(\xi = 1)$ and its reflected image $(\xi = \xi_o^2)$:

$$\varphi_1 = -\varphi_2 = \arccos \frac{(1 - \sigma_m)}{\lambda} \tag{57}$$

$$\varphi_3 = -\varphi_4 = \text{arc cos}\,\frac{(\xi_o{}^2 - \sigma_m)}{\lambda} \tag{58}$$

On the arc between φ_1 and φ_2, which contains $\varphi = 0$, and on the arc between φ_3 and φ_4, which contains $\varphi = \pi$, the normal component is zero; on the remaining circumference - i.e., between φ_1 and φ_3, and between φ_2 and φ_4, it has the value conformable to equations (5) and (52). From these boundary conditions, equations (53) and (52) give the radial velocity at:

$$\left.\begin{aligned} w_{II} &= \frac{v\,k}{2\pi\,\sin\varphi}\left[\int_{\varphi_1}^{\varphi_3} \frac{\sin\psi}{\sigma_m + \lambda\cos\psi}\cot\frac{\varphi - \psi}{2}\,d\psi + \right. \\ &\qquad \left. + \int_{\varphi_4}^{\varphi_2} \frac{\sin\psi}{\sigma_m + \lambda\cos\psi}\cot\frac{\varphi - \psi}{2}\,d\psi\right] \\ &= \frac{vk}{\pi}\left[\frac{1}{\sqrt{2\xi\,\sigma_m - \xi_o{}^2 - \xi^2}}\left(\varphi_3 - \varphi_1 - \frac{2\xi_o}{\xi}\right)\text{arc tan}\,\frac{1-\xi_o}{\sqrt{\sigma - 1}} + \right. \\ &\qquad \left. + \frac{1}{\xi}\ln\left|\frac{\sin\frac{\varphi_3 - \varphi}{2}\,\sin\frac{\varphi_1 + \varphi}{2}}{\sin\frac{\varphi_1 - \varphi}{2}\,\sin\frac{\varphi_3 + \varphi}{2}}\right|\right] \end{aligned}\right\} \tag{59}$$

with $\varphi = \text{arc cos}\,(\xi - \sigma_m)/\lambda$ in the last term. Therefrom integration gives the circulation Γ according to equation (2). But this integral can no longer be expressed in closed formula and must be mathematically evaluated.

The values obtained for one vane can be transferred to n vanes by conformal transformation. The result is shown in figures 15 to 21.

On contra-vanes terminating at or inside the jet boundary, it is immaterial - as far as the circulation distribution is concerned - how far the jet extends beyond the guide vanes. For such cases the circulation distribution can be generalized by using the outside radius of the contra-vane $s = \sigma R$ as unit of the abscissa instead of the jet radius R. Thus, figures 15 to 17 show ξ/σ as abscissa instead of ξ.

As in the case of a contra-vane with infinitely long blades (equation 39), the thrust gain and hence the maximum theoretical vane efficiency η_m is obtained from the circulation distribution (figs. 22 to 25).

EFFECT OF DRAG ON BEST VANE LENGTH

According to the foregoing calculations, the outer parts of the vanes still contribute appreciably to energy recovery. But for constructive reasons, the vanes are made as short as possible and part of this energy gain relinquished. But even if no constructive points of view are involved, it will not be possible to utilize the energy gain due to the outer vane portions, for guide vanes also offer resistance, and for vane portions too far outside, the resistance losses are greater than the theoretical gain. It may therefore be of interest to ascertain the proper length of the vanes without restrictions through design reasons and the amount of energy loss if made shorter.

The tangential components of the spiral motion u being assumed small compared to forward speed v $(u << v)$, the lift of a vane element follows at

$$d\,A = \rho\, v\, \Gamma\, dr \tag{60}$$

drag/lift

With ϵ as the lift/drag ratio of the profile, the drag of the element becomes

$$dW = \epsilon\, d\,A = \epsilon\, \rho\, v\, \Gamma\, dr \tag{61}$$

For the n vanes, the total drag is

$$W = n\, \epsilon\, \rho\, v \int_{r_o}^{s} \Gamma\, dr = 2\rho\, R^2\, \pi\, v^2\, k\, \epsilon \int_{\xi_o}^{\sigma} \frac{n\Gamma}{\Gamma_o}\, d\,\xi \tag{62}$$

(ϵ was assumed constant for all vane elements).

The thrust gain is according to equations (45) and (44):

$$\delta S = \delta\ S_o\ \eta_m = \rho\left(R^2\ \pi\ v^2\right) k^2\ \eta_m\ \ln \frac{1}{\xi_o} \tag{63}$$

hence the contra-vane efficiency

$$\eta = \frac{\delta S - W}{\delta\ S_o} = \eta_m - \frac{2\epsilon}{k}\ \psi \tag{64}$$

whereby

$$\psi = \frac{1}{\ln \frac{1}{\xi_o}} \int_{\xi_o}^{\sigma} \frac{n\Gamma}{\Gamma_o}\ d\xi \tag{65}$$

Figures 26 to 37 show ψ and η for different values of

$$\frac{2\epsilon}{k} = \frac{4\ \epsilon\ \eta_p}{\lambda\ c_s}$$

plotted against the radius of the vane tip σ.

The propeller thrust is, according to equations (6), (7), and (44):

$$S = \frac{\rho}{2}\left(R^2\ \pi\ v^2\right) c_s = \rho\ R^2\ \pi\ v^2\ \eta_p\ \frac{k}{\lambda} = \frac{\eta_p}{k\lambda}\ \frac{\delta S_o}{\ln \frac{1}{\xi_o}} \tag{66}$$

Hence the ratio of thrust gain to thrust is

$$\frac{\delta S - W}{S} = k\ \lambda\ \frac{\eta}{\eta_p}\ \ln \frac{1}{\xi_o} \tag{67}$$

and the gain in total efficiency

$$\delta\eta = \frac{\delta S - W}{S}\ \eta_p = k\ \lambda\ \eta\ \ln \frac{1}{\xi_o} \tag{68}$$

These quantities are reproduced as far as factor $\frac{k\lambda}{\eta_p} \ln \frac{1}{\xi_o}$ and $k\ \lambda\ \ln \frac{1}{\xi_o}$, respectively, in figures 26 to 37.

EFFECT OF HUB DIAMETER

As the hub diameter of the contra-vane may differ from that of the propeller (figs. 38 and 39), its diameter can be freely chosen, and this introduces the problem of suitable diameter. According to figures 22 to 25, the efficiency approaches 1 as the hub ratio ξ_o decreases, making it appear as if a minimum hub diameter were desirable. But this conclusion is wrong. The high efficiency is due to the fact that the great spiral energy is well utilized at small radii r. With a large hub this great spiral energy is altogether avoided, thus obviating its utilization in the first place.

If r_p is the hub radius of the propeller and R_p the correlated jet radius; r_o and R the hub and jet radius at the contra-vane; and r_x and R_x the corresponding values at any intermediate point, we find by reason of the condition of constant section,

$$R^2 - r_o^2 = R_x^2 - r_x^2 = R_p^2 - r_p^2 \tag{69}$$

The spiral distribution, independent of the radial displacement of the fluid, is always given through the same relation, $u = v\,k\,\frac{R}{r}$; only it extends directly behind the propeller from r_p to R_p, and after transition, from r_o to R. The spiral energy per unit length of jet before transition, is

$$E_1 = \int_{r_p}^{R_p} \frac{\rho}{2} u^2\, 2r\,\pi\, dr = \rho\, v^2\, k^2\, R^2\, \pi \ln \frac{R_p}{r_p} \tag{70}$$

and

$$E_2 = \rho\, v^2\, k^2\, R^2\, \pi \ln \frac{R}{r_o} \tag{71}$$

after transition.

A reduction in hub diameter behind the propeller (fig. 39), raises the kinetic energy of the spiral motion. This growth of energy is attributable to the fact that on the transition piece the pressures cause an axial force component contrary to the direction of motion (additional drag), the counteraction of which requires energy. The pressure at radius r_x is:

$$p_x = p_o - \rho \int_{r_x}^{R_x} \frac{u^2}{r}\, dr = p_o - \frac{\rho}{2} v^2 k^2 R^2 \left(\frac{1}{r_x{}^2} - \frac{1}{R_x{}^2}\right) \quad (72)$$

where p_o = pressure outside of the jet. The axial force component following from these pressures is:

$$P = \int_{r_o}^{r_p} (p_o - p_x)\, 2r_x\, \pi\, dr_x \quad (73)$$

Since $R_x = \sqrt{R^2 - r_o{}^2 + r_x{}^2}$, according to equation (69), we find, according to (72) and (73),

$$P = \rho\, v^2\, k^2\, R^2\, \pi \ln \frac{R\, r_p}{r_o \sqrt{R^2 - r_o{}^2 + r_p{}^2}} = E_2 - E_1 \quad (74)$$

Hence the diminution of the hub requires an additional energy Pv per second, which appears in raised spiral energy and is, in part, recovered by the contra-vane. This method is obviously less economical than not making the hub smaller.

From this point of view it is, in fact, more appropriate to make the hub of the contra-vane as large as possible, as then the low pressures at the transition give a propulsion, through which a substantial part of the rotational motion is already recovered, so that the work of the guide vanes is reduced to a small fraction. Admittedly, it must be borne in mind that the hub itself offers resistance which becomes so much higher as the hub is larger. Hence the utilization of the advantages of a large hub is contingent upon the pressure of a thick body (fuselage, engine nacelle) behind the propeller, in which case the guide vanes are best attached to the thickest part of this body.

Translation by J. Vanier,
National Advisory Committee
for Aeronautics.

REFERENCES

1. Betz, A.: Schraubenpropeller mit geringstem Energieverlust (Prandtl-Betz, Vier Abhandlungen zur Hydrodynamik und Aerodynamik, Göttingen, 1927 (Auslieferung durch Julius Springer, Berlin)).

2. Hütte, Bd. I, S. 405. 26. Aufl.

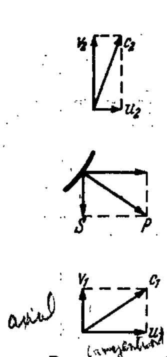

Figure 1.- Action of guide vanes.

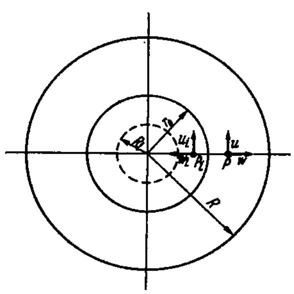

Figure 2.- Reflection at hub.

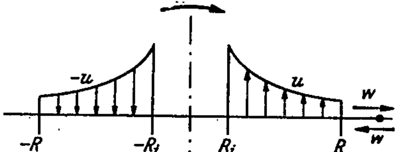

Figure 3.- Normal and tangential velocity component on the infinitely long vanes of a 2 blade contra-vanes

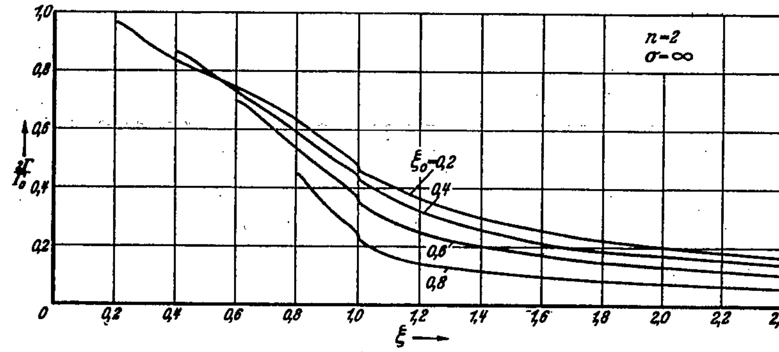

Fig. 5

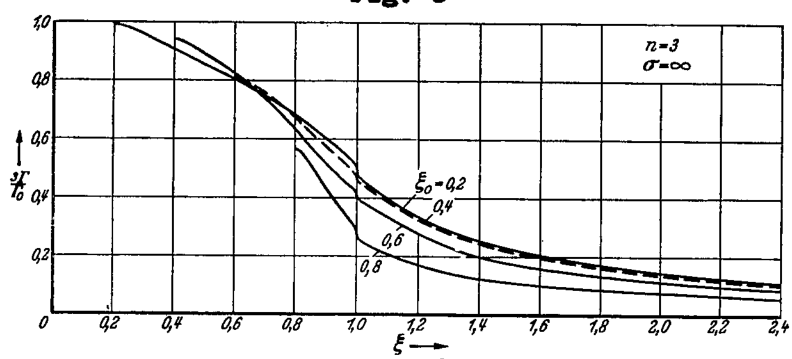

Fig. 6

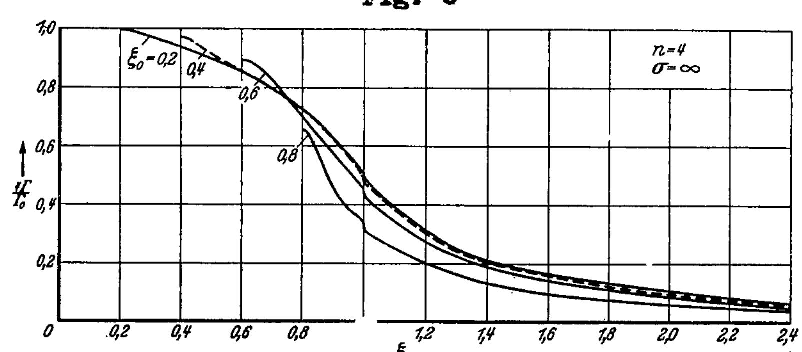

Fig. 7

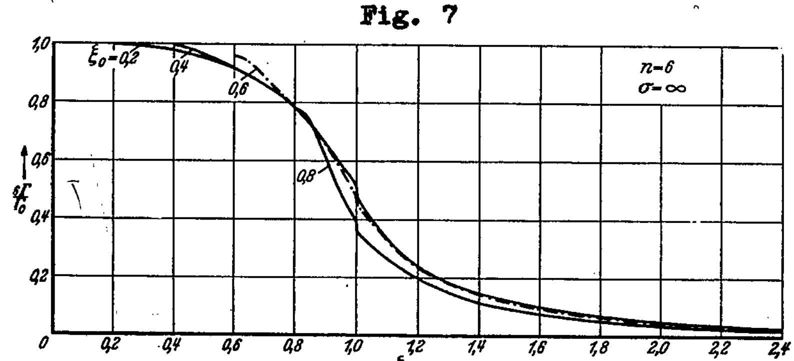

Fig. 8

Figures 5-8.- Best circulation distribution on contra-vanes with 2,3,4 and 6 blades of infinite length at different hub ratios.

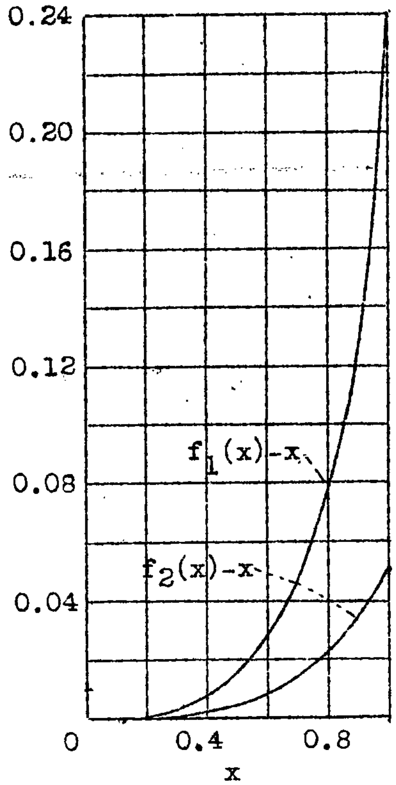

Figure 4.- Two auxiliary formations.

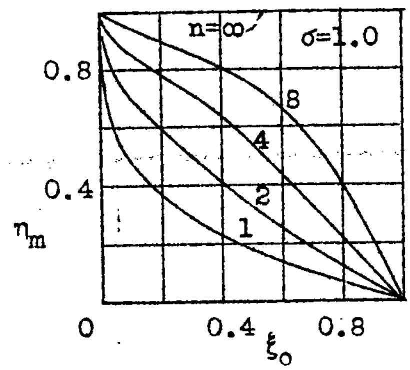

Figure 22.-Maximum theoretical efficiency of contra-vanes terminating at jet boundary,for different blade numbers.

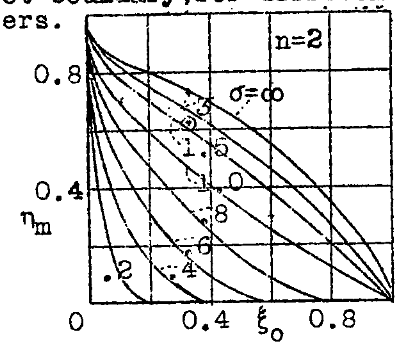

Figure 23

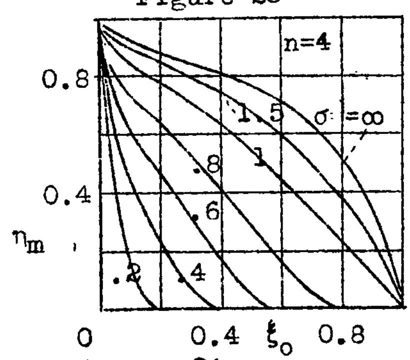

Figure 24

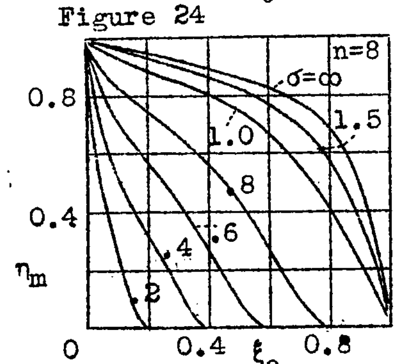

Figure 25

Figures 23 to 25.-Maximum theoretical efficiency of contra-vanes of different diameters with 2,4 or 8 blades.

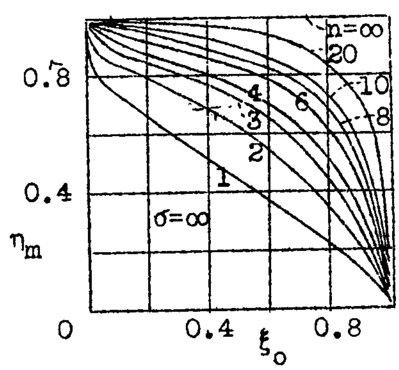

Figure 13.- Maximum theoretical efficiency of contra-vanes with different blade numbers and infinite blade length.

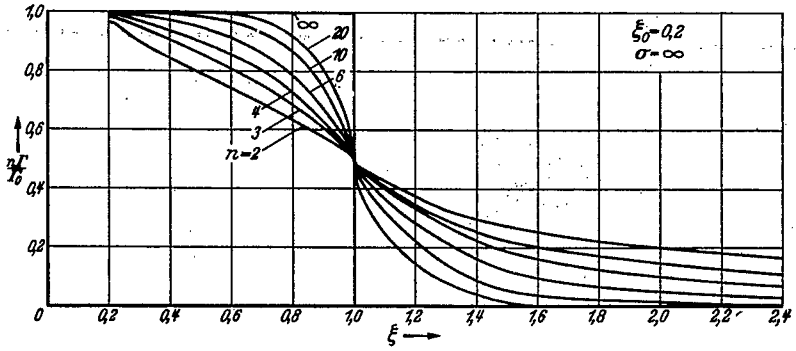

Fig. 9

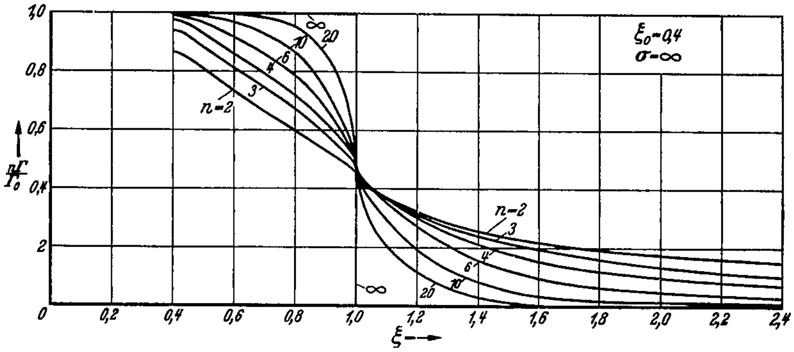

Fig. 10

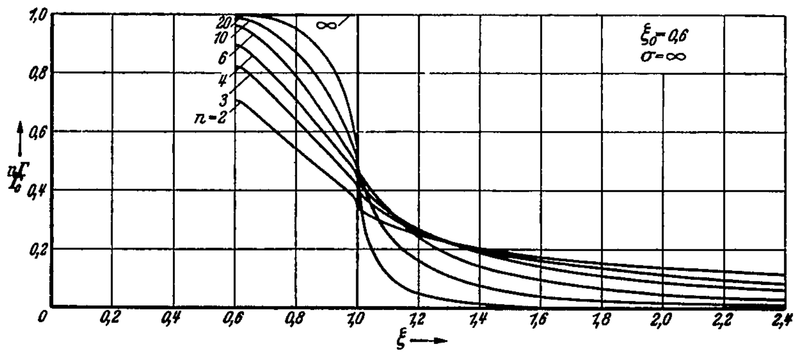

Fig. 11

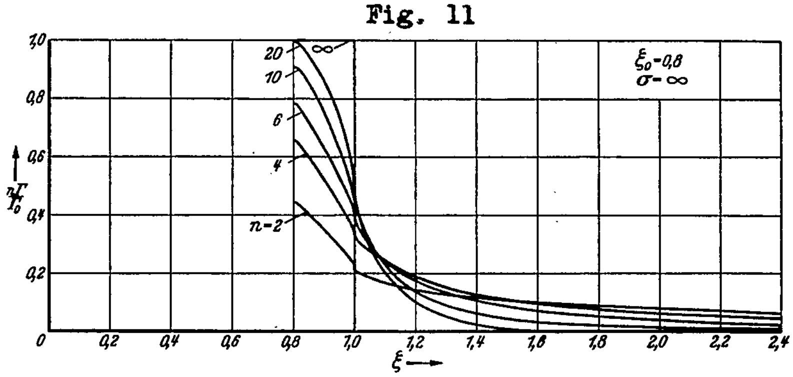

Fig. 12

Figure 9-12.- Best circulation distribution with contra-vanes of hub ratio ξ_0=0.2, 0.4, 0.6, 0.8, at different blade numbers and infinite blade length.

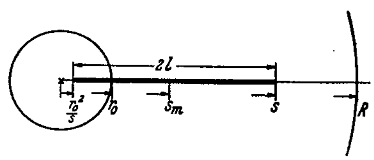

Figure 14.- Single blade of limited length and its reflection at the hub.

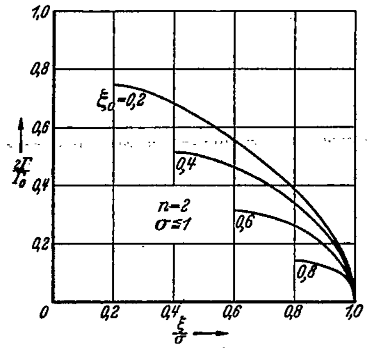

Fig. 15

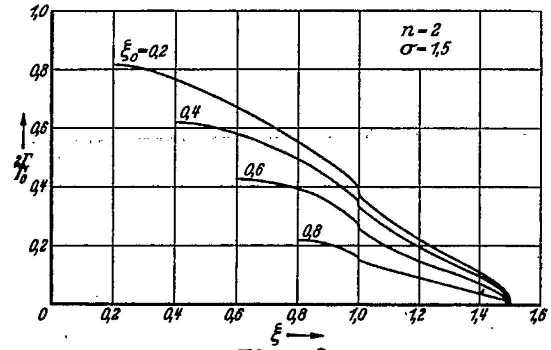

Fig. 18

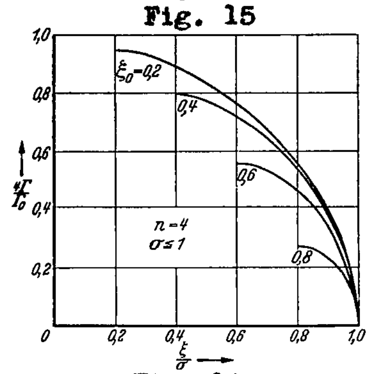

Fig. 16

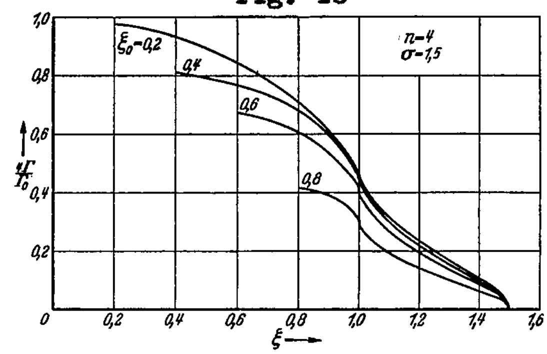

Fig. 19

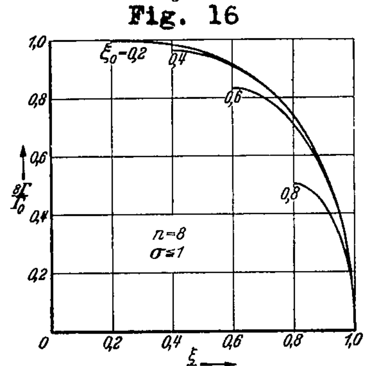

Fig. 17

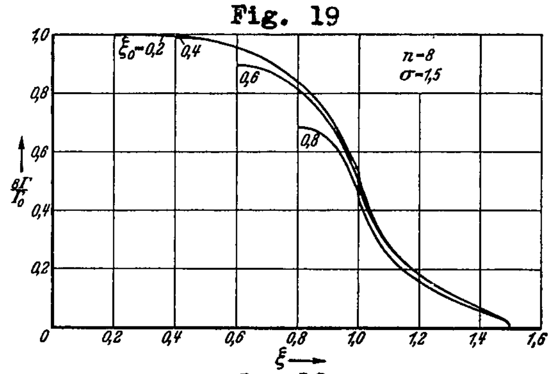

Fig.20

Figures 15-17.- Optimum circulation distribution on contra-vanes of 2,4, and 8 blades terminating at or within the jet boundary for different hub ratios.

Figures 18-20.- Optimum circulation distribution on contra-vanes of 2,4, and 8 blades extending up to 1.5 R for different hub ratios.

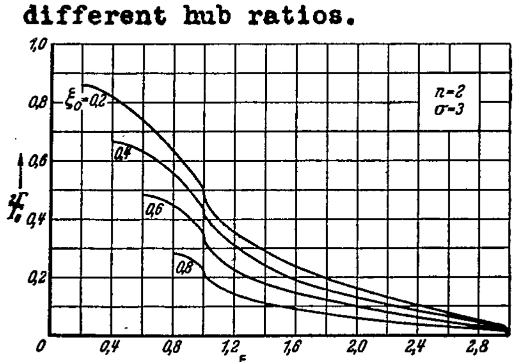

Figure 21.- Optimum circulation distribution on contra-vanes with two blades extending to 3 R.

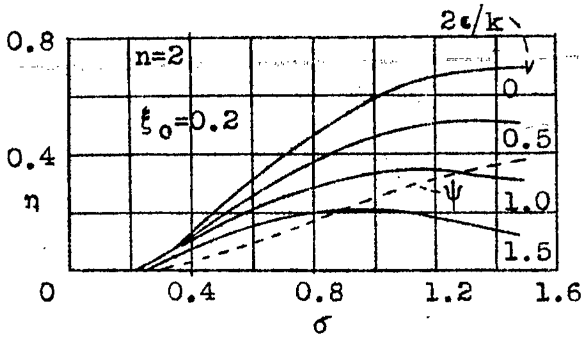

Figure 26

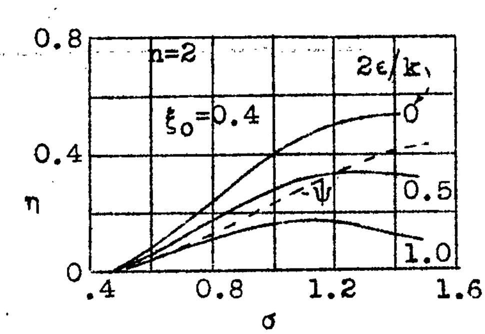

Figure 29

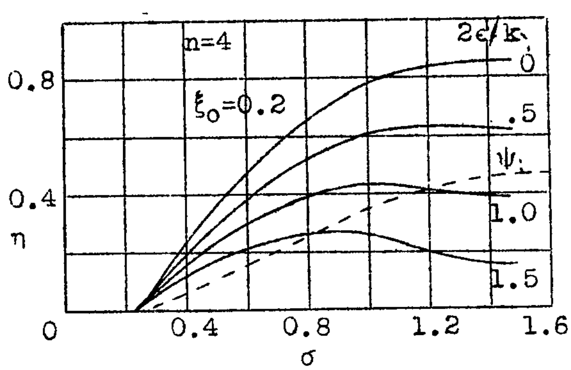

Figure 27

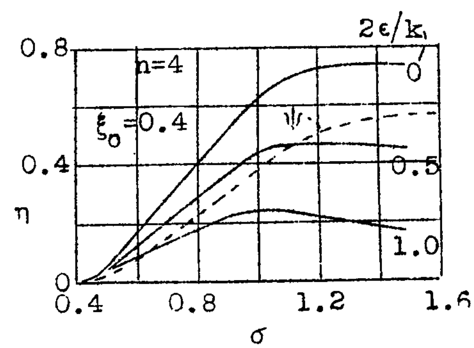

Figure 30

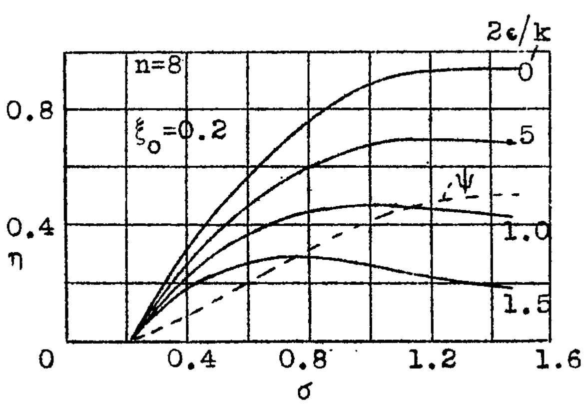

Figure 28

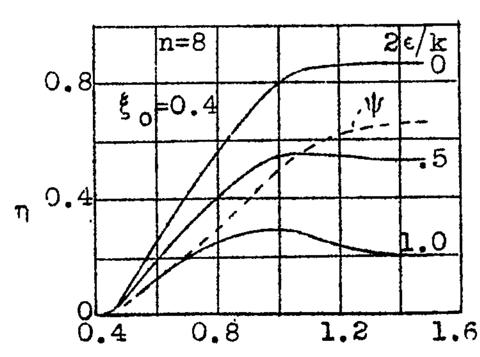

Figure 31

Figures 26-31.- Efficiency of contra-vanes with allowance for blade ϵ.

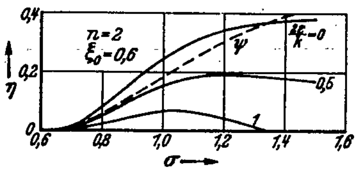

Fig. 32

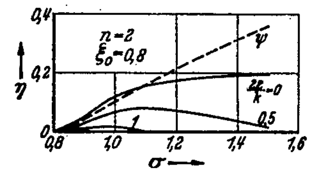

Fig. 35

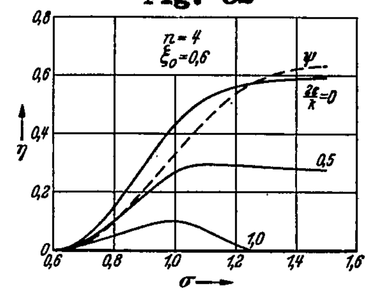

Fig. 33

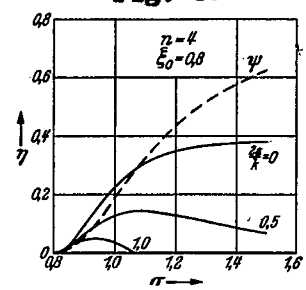

Fig. 36

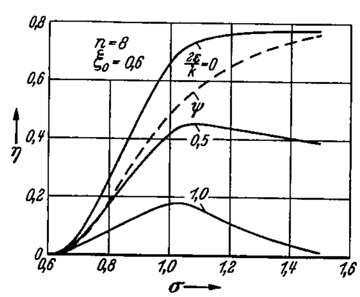

Fig. 34

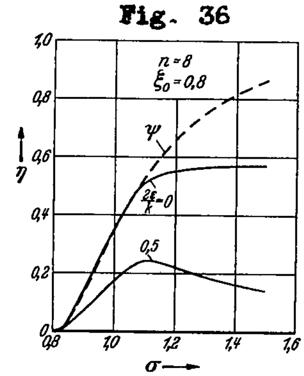

Fig. 37

Figures 32-37.- Efficiency of contra-vanes with allowance for blade ϵ.

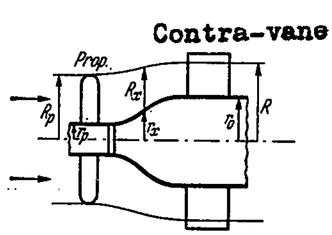

Fig. 38

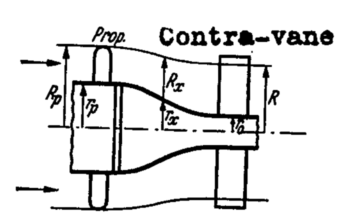

Fig. 39

Figures 38-39.- Arrangements on which the hub diameter between propeller and contra-vanes increases or decreases.